



Published in final edited form as:

*Int J Cardiovasc Imaging*. 2016 May ; 32(5): 817–823. doi:10.1007/s10554-015-0831-7.

## Correlation Of CT-Based Regional Cardiac Function (SQUEEZ) With Myocardial Strain Calculated From Tagged MRI: An Experimental Study

Amir Pourmorteza, Ph.D.<sup>\*</sup>, Marcus Y. Chen, M.D.<sup>†</sup>, Jesper van der Pals, M.D., Ph.D.<sup>†</sup>, Andrew E. Arai, M.D.<sup>†</sup>, and Elliot R. McVeigh, Ph.D.<sup>††</sup>

<sup>\*</sup>Radiology and Imaging Sciences, National Institutes of Health Clinical Center, Bethesda, MD, USA

<sup>†</sup>Advanced Cardiovascular Imaging Laboratory, Cardiopulmonary Branch National Heart Lung and Blood Institute, National Institutes of Health, Bethesda, MD, USA

<sup>††</sup>Department of Bioengineering, University of California, San Diego, CA, USA

### Abstract

**Purpose**—The objective of this study was to investigate the correlation between local myocardial function estimates from CT and myocardial strain from tagged MRI in the same heart. Accurate detection of regional myocardial dysfunction can be an important finding in the diagnosis of functionally significant coronary artery disease. Tagged MRI is currently a reference standard for noninvasive regional myocardial function analysis; however, it has practical drawbacks. We have developed a CT imaging protocol and automated image analysis algorithm for estimating regional cardiac function from a few heartbeats. This method tracks the motion of the left ventricular (LV) endocardial surface to produce local function maps: we call the method Stretch Quantification of Endocardial Engraved Zones (SQUEEZ).

**Methods**—Myocardial infarction was created by ligation of the left anterior descending (LAD) coronary artery for 2 hours followed by reperfusion in canine models. Tagged and cine MRI scans were performed during the reperfusion phase and first-pass contrast enhanced CT scans were acquired. The average delay between the CT and MRI scans was <1 hour. Circumferential myocardial strain (Ecc) was calculated from the tagged MRI data. The agreement between peak systolic Ecc and SQUEEZ was investigated in 162 segments in the 9 hearts. Linear regression and Bland-Altman analysis was used to assess the correlation between the two metrics of local LV function.

**Results**—The results show good agreement between SQUEEZ and Ecc: ( $r = 0.71$ , slope = 0.78,  $p < 0.001$ ). Furthermore, Bland-Altman showed a small bias of  $-0.02$  with 95% confidence interval of 0.1, and standard deviation of 0.05 representing ~6.5% of the dynamic range of LV function.

---

Address for correspondence: Amir Pourmorteza, PhD, 10 Center Dr., Bethesda, MD, 20892, Tel/fax: +1-443-799-8339, amir.pourmorteza@nih.gov.

#### Compliance with Ethical Standards

Ethical approval: All applicable international, national, and/or institutional guidelines for the care and use of animals were followed.

Conflict of interest: Drs. Pourmorteza and McVeigh are inventors on a pending patent for SQUEEZ (WO Patent 2013056082)

**Conclusion**—The good agreement between the estimates of local myocardial function obtained from CT SQUEEZ and tagged MRI provides encouragement to investigate the use of SQUEEZ for measuring regional cardiac function at a low clinical dose in humans.

## Keywords

Myocardial function; Tagged MRI; Contractility; CT SQUEEZ

---

## Introduction

Accurate detection and estimate of the extent of regional myocardial dysfunction is important in the diagnosis and management of patients with coronary artery disease (CAD) [1].

Recent developments in coronary CT angiography (CTA) technologies provide images with exceptionally high sensitivity for detection and visualization of culprit lesions and a high negative predictive value for exclusion of obstructive coronary artery disease[2–5]. The use of CTA in the workup for low to medium risk patients with chest pain has been shown to be equally predictive of future events at two years as standard stress testing [6]. These techniques are extremely robust and require only 1 to 3 heartbeats depending on the generation of CT scanner that is used.

The assessment of *resting* left ventricular (LV) function with CT has been shown to improve the diagnostic accuracy of acute coronary syndrome (ACS) in patients suffering from chest pain; Results of the ROMICAT trial indicated that adding regional LV function resulted in 10% increase in sensitivity to detect ACS by cardiac CT in these patients and significantly improved the overall accuracy [1].

Recently, Stretch QUantification of Endocardial Engraved Zones (SQUEEZ) has been introduced as a method for quantitative assessment of left ventricular function by automatic 3D tracking of structures on the endocardial surface[7, 8]. This method rapidly produces high spatial resolution estimates of local myocardial function without the need for contouring the endocardium or epicardium.

In this paper we assess the agreement between SQUEEZ calculated from CT and circumferential strain, calculated from tagged MRI in the same heart in an acute model of myocardial infarction in ten canines.

## Methods

### 1.1. Animal Model

Ten dogs weighing 10 to 15 kg were studied with institutional approval. Anesthesia was induced by subcutaneous acepromazine (0.2 mg/kg), followed by intravenous thiopental sodium (15 mg/kg). Anesthesia was sustained by inhaled isoflurane (0.5% to 2.0%). A model of acute myocardial infarction was created; the animals were intubated and surgical preparation included median sternotomy, venous catheters, arterial lines, and a snare around the left anterior descending (LAD) coronary artery, typically positioned distal to the first

diagonal branch. The LAD was then occluded for two hours followed by at least 1.5 hours of reperfusion prior to commencing MR imaging. After the MRI scans, the animals were transported to the CT suite. The LAD was re-occluded less than 5 minutes prior to contrast injection and CT scan. The average delay between the MRI and CT scans was less than one hour. The animals were euthanized after the scans. Measurement of SQUEEZ with CT and myocardial tagging with MRI were in addition to perfusion measurements obtained in the same animals for another experiment not reported here. All animal studies were approved by institutional animal care and use committee and comply with the Guide for the care and Use of Laboratory Animals (National Institutes of Health Publication no. 80-23, revised 1985).

## 1.2. MRI Acquisition

The MRI studies were started after a period of 1.5 hours of reperfusion, during which time the animals were stabilized. The exams were conducted on a 3-T scanner (Magnetom Skyra, Siemens Healthcare Sector, Erlangen, Germany) in a supine position, with ECG triggering, dedicated cardiac surface coils and expiratory breath holds. We acquired 2D cine MRI using a cardiac gated steady state free precession (True-FISP) sequence in a stack of short-axis slices. Next a gradient echo short-axis tagging sequence was used to acquire tagged myocardial tissue images. Typical scan parameters tagging were as follows: TR/TE=46.25/4.20, flip angle=14°, acquisition matrix= 256 × 168, pixel size and slice thickness= 1.05 × 1.05 × 8 mm. Tagged images were acquired for the first ~60% of the cardiac cycle capturing all of systole.

## 1.3. CT Acquisition

Animals were scanned with ECG monitoring using a 320-row detector scanner (Aquilion ONE VISION; Toshiba Medical Systems Corporation, Otawara, Japan). First-pass contrast enhanced CT scans were acquired while respiration was suspended using a 3 to 5-beat retrospectively gated protocol with the following x-ray tube parameters: 80 kVp and 600 mA. Gantry rotation speed (275 ms – 350 ms) was set based on the animal's heart rate to ensure optimal temporal resolution (40–60 ms). Real-time bolus tracking was performed using Toshiba's SUREstart following a bolus injection of 35 to 60 ml of iodixanol (Visipaque 320, GE Healthcare Inc., Princeton, NJ) at a rate of 1 ml/sec. The scan was triggered when the intensity of the blood in the LV reached 800 HU. In addition, a two-minute delayed contrast enhanced CT was acquired at 75% of the R-R cycle to visualize the infarct region.

CT volumes were reconstructed using the standard setting of the 3D Adaptive Iterative Dose Reduction (AIDR 3D) reconstruction algorithm with the FC08 kernel at 0.5 mm slice thickness and ~0.45 mm in-plane pixel size. A total of 20 volumes were reconstructed at 5% intervals of the R-R cycle. ECG editing was performed when necessary to account for arrhythmias. The images were then manually reoriented into short-axis view using Osirix Imaging software (Pixmeo SARL, Bernex, Switzerland).

## 1.4. Myocardial Function Estimation with SQUEEZ and tagged MRI

Global ejection fraction was calculated from both MRI and CT acquisitions. The LV was manually segmented from the cine MR images using Osirix Imaging Software. In some

animals, the physiological state changed significantly in the time between the MRI and the CT exams.

#### 1.4.1. Calculation of circumferential strain ( $E_{cc}$ ) from tagged MRI—

Circumferential myocardial strain ( $E_{cc}$ ) was estimated by manual segmentation and analysis of the tagged images using FindTags [9] and Tagged Tissue Tracker (TTT) [10] software packages developed at the Johns Hopkins University (Baltimore, MD). FindTags was used to automatically contour the endocardial and epicardial boundaries and segment the tags. The automatically created contours and tags were manually edited. Next, a B-spline-based motion tracking technique (TTT) was used to track the tags and calculate subendocardial circumferential strain. The MR circumferential strain ( $E_{cc}$ ) curves were calculated as the estimate of local LV function.

#### 1.4.2. Calculation of local endocardial strain (SQUEEZ) from CT—

For each systolic cardiac phase in the CT volumes, regional myocardial function was calculated with Stretch QUantification of Endocardial Engraved Zones (SQUEEZ) [7, 8]. The contrast enhanced LV blood was automatically segmented by thresholding the image intensity over a predetermined Hounsfield Unit (~250HU), followed by manual selection of the level of the mitral valve in the end-diastolic and end-systolic short-axis slices. This yielded a set of 3D “casts” with the details of the LV endocardial structures (ex. the trabeculae and papillary muscles) engraved on each cast. A 4D non-rigid deformation algorithm was then used to warp the end-diastolic cast into the shape of the subsequent casts through the heart cycle. The resulting deformation fields were used to precisely calculate the local wall motion and contraction at all sampled points on the LV endocardium. The method is described in detail in Pourmorteza et al [7].

A SQUEEZ value of 0.75 means the tissue has contracted 25% (normal), a value of 1.0 means the tissue is akinetic, and a value of 1.25 means the tissue has stretched by 25% (dyskinetic). On the other hand, strain metrics derived from tagged MRI, such as circumferential shortening ( $E_{cc}$ ) are represented as percentage of stretch (for example,  $E_{cc} = -0.25$  in normal tissue,  $E_{cc} = 0$  in akinetic tissue, and  $E_{cc} = 0.25$  in dyskinetic tissue). Since there is an offset of 1 between the SQUEEZ and  $E_{cc}$  metrics, we compared  $E_{cc}$  to SQUEEZ-1 throughout this paper. The SQUEEZ vs. time and  $E_{cc}$  vs. time curves were computed in an 18-segment bull’s-eye plot of the left ventricle; The LV was divided into 3 short-axis sections (basal, mid-cavity, apical) along the long-axis direction with each short-axis section divided into 6 equal angular segments (Fig. 1). Peak systolic SQUEEZ and  $E_{cc}$  contraction values were compared for each segment in the bull’s-eye plots. In addition, we selected regions of roughly the same size (3 AHA segments) in the infarct zone (MI), peri-infarct zone (PIZ), and remote myocardium. The regions were chosen based on the corresponding 2-minute delayed enhanced short-axis CT images of each animal (Fig. 2); PIZ was defined as the region covering a 30° sector of the myocardium in short-axis slices adjacent to both borders of the infarct area consistent with the segmentations reported in [11, 12]. The peak systolic contraction values calculated from CT and MRI were compared in each region for all animals.

## 1.5. Statistical Analysis

Comparisons between peak systolic LV contraction values by SQUEEZ and tagged MRI were performed by linear regression analysis between (SQUEEZ-1) vs.  $E_{cc}$ . Differences between myocardial peak systolic strains were assessed and the agreement between the two methods (peak systolic function by Ecc and SQUEEZ-1) was expressed as 95% limits of agreement, as recommended by Bland and Altman[13]. Differences in myocardial function between the MI, PIZ, and remote regions were tested using one-way analysis of variance (ANOVA) with post-hoc pairwise comparison of CT and MR values using paired Student's t-test. Statistical significance level was set at  $p < 0.05$ .

## RESULTS

For each heart the global LV function was calculated; Table-2 gives the global ejection fraction (EF) values for each animal computed from the MRI and CT acquisitions. The heart rates of the animals were in the 80–130 bpm range. One animal was excluded due to motion artifacts in the CT acquisition caused by spontaneous respiratory motion. In the remaining 9 animals, SQUEEZ and  $E_{cc}$  were calculated at all systolic phases and the peak contraction values were extracted from the time plots (Fig. 1) in a total of 162 LV segments. The average processing time, including manual segmentation and processing, for each heart was less than 6 minutes for SQUEEZ for a reader with more than 6 years of experience in analyzing cardiac CT and MR images; this was considerably less than the time required to edit contours and tags using FindTags and TTT. The range of the (SQUEEZ - 1) values was  $-0.31$  to  $-0.01$ , and the range of the Ecc values was  $-0.26$  to  $+0.01$ . The peak contractions from SQUEEZ were then compared to the peak  $E_{cc}$  from tagged MRI on a segment by segment basis (Fig. 3). Linear regression analysis showed good correlation between (SQUEEZ-1) and  $E_{cc}$ :  $r=0.71$ ,  $p<0.001$ , slope= $0.78$ , intercept=  $-0.05$ .

The Bland-Altman analysis of the results yielded bias of  $-0.02$  (with SQUEEZ showing the slight bias towards more contraction) and a 95% confidence interval  $\pm 0.10$  (standard deviation= 0.05). Figure 4 demonstrates the comparison between SQUEEZ and  $E_{cc}$  in infarcted (MI), PIZ, and remote regions of the myocardium for all 9 animals (N=18 segments in each region). No statistically significant difference was found between CT and MRI myocardial function estimates in each region. The myocardial function showed statistically significant decrease starting from the remote region, to the PIZ, and to the MI region with  $p<0.001$ . This was consistent with the previous reports of myocardial dysfunction in peri-infarct zone [12].

## Discussion

Tagged MRI is a highly attractive tool for assessing myocardial viability and cardiac function analysis. However, it has some practical drawbacks compared to CT, including higher cost, complicated image acquisition and analysis, and long scan times with multiple breath-holds. Another significant difference between MRI and CT is the lack of ability to perform a highly reproducible, high-resolution coronary angiogram during the study.

Present CT-based methods of regional LV function assessment either rely on manual contouring of the endocardial and epicardial borders of the left ventricle or are based on subjective visual scoring of the motion and/or shortening of the LV wall [14, 15]. These 2D analysis methods are also susceptible to error from through-plane motion artifacts. In addition the modest performance of texture feature-tracking methods, originally designed for echocardiography speckle tracking, compared to tagged MRI [16] can be attributed to the differences in the physics of noise between the two modalities; unlike in ultrasound images where noise texture is reflective of background tissue structure, the CT noise is non-stationary and spatially variant; therefore, tracking texture features in CT is not necessarily the same as tracking the “noiseless” myocardium.

Here we automatically segmented the endocardial boundary between the high-contrast blood pool and the myocardium, which is more robust to noise, and tracked its in 3D to avoid the lengthy manual contouring step and eliminate through-plane motion artifacts. The automatic segmentation is done readily using a global thresholding method as described in [7].

### **SQUEEZ vs. MRI strain**

Despite the fact that CT SQUEEZ and tagged MRI do not measure precisely the same metrics of regional function, SQUEEZ and  $E_{cc}$  were highly correlated and the standard deviation of the difference between them was very small (6.5% of the dynamic range of the measurements). There are a few possible sources of the observed differences between  $E_{cc}$  and SQUEEZ:

1. Although both SQUEEZ and  $E_{cc}$  measure local cardiac wall deformation, they are different physical entities;  $E_{cc}$  is a measure of subendocardial myocardial contraction in the circumferential direction, whereas SQUEEZ is a directionless measure of the geometric mean of contraction on the endocardial *surface*.
2. The  $E_{cc}$  measurements from myocardial tagging are not conducted on the endocardial surface, they are an average over an ~8mm thick slice from the subendocardial to the midwall region of myocardium. Consequently, the underlying true relationship between  $E_{cc}$  and SQUEEZ-1 may not be linear with a slope of 1, because of the transmural decrease of local shortening from endocardium to epicardium in the LV [17]. We anticipated that SQUEEZ would measure a higher amount of contraction and this was observed.
3. Cardiac CT images are typically acquired in 1–3 heartbeats in a single breath-hold; the tagged MRI acquisitions in this study, however, took 20 heartbeats for each of 8 short-axis slices (8 breath-holds). Therefore tagged MRI provides measurements that are averaged over ~160 heartbeats; SQUEEZ on the other hand is less susceptible to the intrinsic temporal variability in stroke volume and heart rate.

### **Choice of an acute model of infarction**

Although we tried to minimize the delay between MRI and CT scans, some difference in strain can be expected during such a dynamic process of coronary reperfusion, as seen globally in the EF measurements. We believe this is close replication of emergent cardiac CT scans performed in the clinic both in terms of the hemodynamic state and the shape of



the ventricle. A chronic model of myocardial infarction, with a more stable hemodynamic state, may be a more convenient model for the side-by-side comparison of the non-tagged MR vs. CT based metrics; however, ventricular remodeling after infarction can confound tagged MR measurements because the thickness of the infarcted LV wall segments are often reduced making it difficult to sample the tissue with a tagging grid. The model used in this study yielded a good dynamic range of contraction state in each heart. Also, this model was available for this study because the acute ischemia was being created to measure other effects not reported in this paper.

Recent advances in CT technology have made it possible to take “snapshots” of the heart with effective doses as low as 0.1 mSv [20] for coronary angiography. The image quality necessary for wall motion tracking can be far lower than that for characterizing the coronary vessels. We have previously shown that by lowering the x-ray tube current and voltage (to ~30 mA and 80 kVp) and using advanced reconstruction algorithms it is possible to calculate reliable SQUEEZ values and reduce the radiation dose 5 to 10-fold [7].

We believe the results of the present study provide encouragement to investigate the use of SQUEEZ as a fully 3D, automatic technique for measuring regional cardiac function in humans at rest. With improved CT acquisition techniques for high heart rate imaging, we believe this technique can be extended to stress testing with functional CT.

## Acknowledgments

Grant sponsor: This research was supported in part by the Maryland Innovation Initiative grant (115127) titled “Diagnostic Method for Rapid Detection of Significant Coronary Heart Disease”.

## References

1. Seneviratne SK, Truong QA, Bamberg F, Rogers IS, Shapiro MD, Schlett CL, Chae CU, Cury R, Abbara S, Brady TJ, Nagurney JT, Hoffmann U. Incremental diagnostic value of regional left ventricular function over coronary assessment by cardiac computed tomography for the detection of acute coronary syndrome in patients with acute chest pain: from the ROMICAT trial. *Circ Cardiovasc Imaging*. 2010; 3:375–83. [PubMed: 20484542]
2. Cury RC, Feuchtner GM, Battle JC, Peña CS, Janowitz W, Katzen BT, Ziffer JA. Triage of patients presenting with chest pain to the emergency department: implementation of coronary CT angiography in a large urban health care system. *AJR Am J Roentgenol*. 2013; 200:57–65. [PubMed: 23255742]
3. Budoff MJ, Dowe D, Jollis JG, Gitter M, Sutherland J, Halamert E, Scherer M, Bellinger R, Martin A, Benton R, Delago A, Min JK. Diagnostic performance of 64-multidetector row coronary computed tomographic angiography for evaluation of coronary artery stenosis in individuals without known coronary artery disease: results from the prospective multicenter ACCURACY (Assessment by Coro. *J Am Coll Cardiol*. 2008; 52:1724–32. [PubMed: 19007693]
4. Min JK, Leipsic J, Pencina MJ, Berman DS, Koo BK, van Mieghem C, Erglis A, Lin FY, Dunning AM, Apruzzese P, Budoff MJ, Cole JH, Jaffer FA, Leon MB, Malpeso J, Mancini GB, Park SJ, Schwartz RS, Shaw LJ, Mauri L. Diagnostic accuracy of fractional flow reserve from anatomic CT angiography. *JAMA*. 2012; 308:1237–1245. [PubMed: 22922562]
5. Al-Mallah MH, Qureshi W, Lin FY, Achenbach S, Berman DS, Budoff MJ, Callister TQ, Chang HJ, Cademartiri F, Chinnaiyan K, Chow BJ, Cheng VY, Delago A, Gomez M, Hadamitzky M, Hausleiter J, Kaufmann PA, Leipsic J, Maffei E, Raff G, Shaw LJ, Villines TC, Cury RC, Feuchtner G, Plank F, Kim YJ, Dunning AM, Min JK. Does coronary CT angiography improve risk stratification over coronary calcium scoring in symptomatic patients with suspected coronary artery

disease? Results from the prospective multicenter international CONFIRM registry. *Eur Hear J Cardiovasc Imaging*. 2013

6. Douglas PS, Hoffmann U, Patel MR, Mark DB, Al-Khalidi HR, Cavanaugh B, Cole J, Dolor RJ, Fordyce CB, Huang M, Khan MA, Kosinski AS, Krucoff MW, Malhotra V, Picard MH, Udelson JE, Velazquez EJ, Yow E, Cooper LS, Lee KL. Outcomes of Anatomical versus Functional Testing for Coronary Artery Disease. *N Engl J Med*. 2015
7. Pourmorteza A, Schuleri KH, Herzka DA, Lardo AC, McVeigh ER. A New Method for Cardiac Computed Tomography Regional Function Assessment: Stretch Quantifier for Endocardial Engraved Zones (SQUEEZ). *Circ Cardiovasc Imaging*. 2012; 5:243–250. [PubMed: 22342945]
8. Pourmorteza A, Schuleri KH, Herzka DA, Lardo AC, McVeigh ER. Regional cardiac function assessment in 4D CT: Comparison between SQUEEZ and ejection fraction. *Engineering in Medicine and Biology Society (EMBC), Annual International Conference of the IEEE*. 2012
9. Guttman MA, Zerhouni EA, McVeigh ER. Analysis of Cardiac Function from MR Images. *IEEE Comput Graph Appl*. 1997; 17:30–38. [PubMed: 18509519]
10. Ozturk C, McVeigh ER. Four-dimensional B-spline based motion analysis of tagged MR images: introduction and in vivo validation. *Phys Med Biol*. 2000; 45:1683–1702. [PubMed: 10870718]
11. Symons R, Masci PG, Goetschalckx K, Doulaptsis K, Janssens S, Bogaert J. Effect of Infarct Severity on Regional and Global Left Ventricular Remodeling in Patients with Successfully Reperfused ST Segment Elevation Myocardial Infarction. *Radiology*. 2014; 274:93–102. [PubMed: 25207466]
12. Inoue Y, Yang X, Nagao M, Higashino H, Hosokawa K, Kido T, Kurata A, Okayama H, Higaki J, Mochizuki T. Peri-infarct dysfunction in post-myocardial infarction: assessment of 3-T tagged and late enhancement MRI. *Eur Radiol*. 2010; 20:1139–1148. [PubMed: 19915846]
13. Bland JM, Altman DG. Measuring agreement in method comparison studies. *Stat Methods Med Res*. 1999; 8:135–160. [PubMed: 10501650]
14. Mahnken AH, Bruners P, Schmidt B, Bornikoel C, Flohr T, Günther RW. Left ventricular function can reliably be assessed from dual-source CT using ECG-gated tube current modulation. *Invest Radiol*. 2009; 44:384–389. [PubMed: 19448556]
15. Nakazato R, Tamarappoo BK, Smith TW, Cheng VY, Dey D, Shmilovich H, Gutstein A, Gurudevan S, Hayes SW, Thomson LEJ, Friedman JD, Berman DS. Assessment of left ventricular regional wall motion and ejection fraction with low-radiation dose helical dual-source CT: Comparison to two-dimensional echocardiography. *J Cardiovasc Comput Tomogr*. 2011; 5:149–157. [PubMed: 21367686]
16. Tee MW, Won S, Raman FS, Yi C, Vigneault DM, Davies-Venn C, Liu S, Lardo AC, Lima JAC, Noble JA. Regional Strain Analysis with Multidetector CT in a Swine Cardiomyopathy Model: Relationship to Cardiac MR Tagging and Myocardial Fibrosis. *Radiology*. 2015; 142339
17. Moore CC, Lugo-Olivieri CH, McVeigh ER, Zerhouni EA. Three-dimensional systolic strain patterns in the normal human left ventricle: characterization with tagged MR imaging. *Radiology*. 2000; 214:453–466. [PubMed: 10671594]
18. Cademartiri F, Maffei E, Arcadi T, Catalano O, Midiri M. CT coronary angiography at an ultra-low radiation dose (<0.1 mSv): feasible and viable in times of constraint on healthcare costs. *Eur Radiol*. 2013; 23:607–613. [PubMed: 23344906]



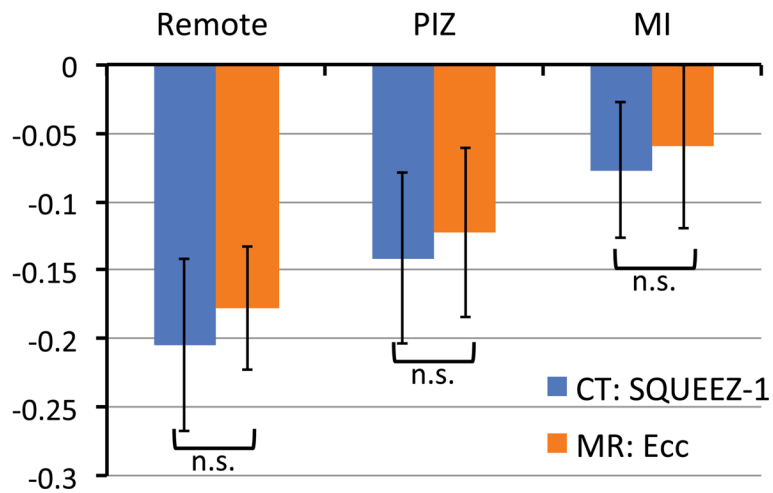


**Figure 1. Tagged MRI, and first-pass CT images used to estimate local myocardial function**  
**A:** Tagged MRI images of a short-axis slice in a canine at end-diastole and end-systole.  
**B:** First-pass CT images of the same animal at end-diastole and end-systole. The dotted lines divide each short-axis slice into 6 angular segments.  
 Time plots during systole of the regional function ( $E_{cc}$ ) of six mid-cavity short-axis segments from tagged MRI (A, right), and regional function from CT (B, right); the x-axis is normalized time from end-diastole through end-systole. The numbers correspond to 1: anterior, 2: anteroseptal, 3: inferoseptal, 4: inferior, 5: inferolateral, and 6: anterolateral segments.

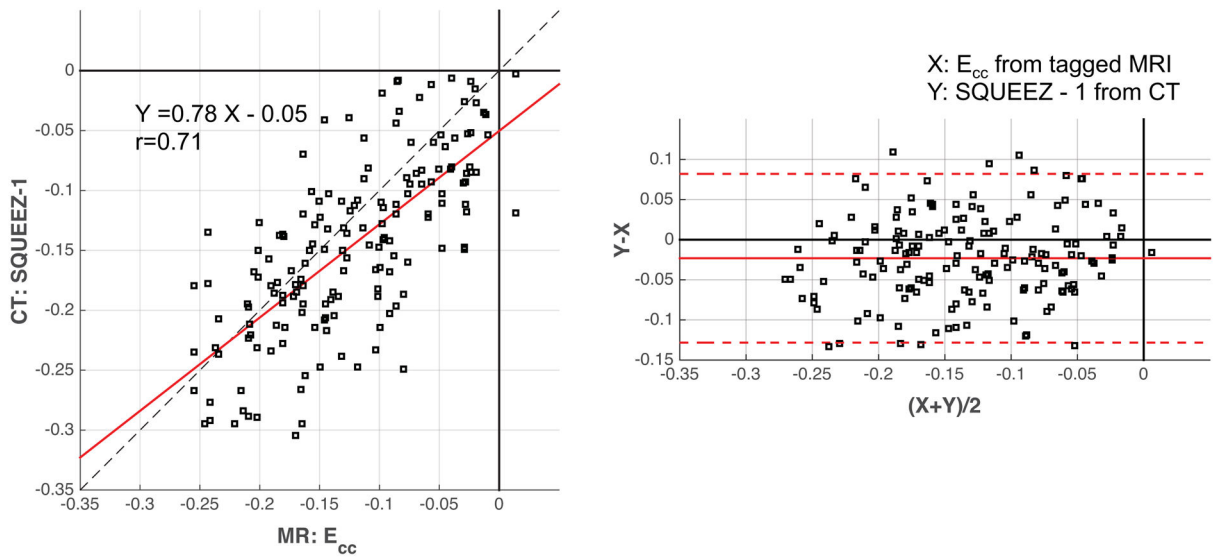


**Figure 2. Delayed contrast-enhance CT image of one animal in A: short-axis view, and B,C: long axis views**

The infarcted region is visible as the hypointense region in the anterior and anterioseptal segments marked by the red arrow. Peri-infarct zone (PIZ) and remote myocardium are shown with yellow and green arrows, respectively.

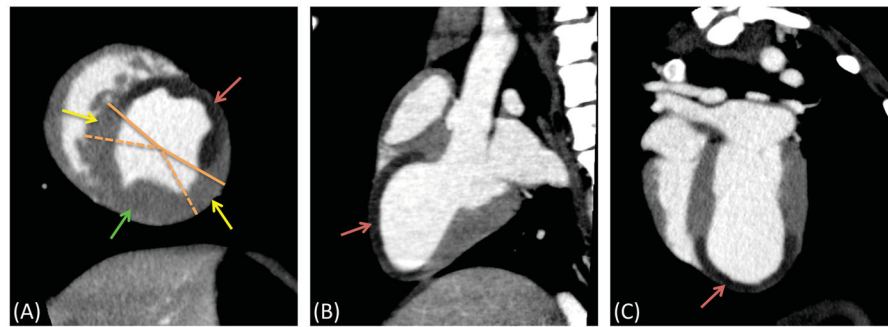


**Figure 3. Correlation of CT and tagged MRI based myocardial function**

**A:** Correlation between peak systolic myocardial function derived from CT (SQUEEZ-1) and tagged MRI ( $E_{cc}$ ) ( $N=162$ , 9 animals  $\times$  18 segments at end-systole); the solid red line represents the linear fit and the dashed line is the line of identity.

**B:** Bland-Altman plot of the agreement between CT (SQUEEZ-1) and tagged MRI ( $E_{cc}$ ) for measuring peak systolic myocardial function ( $N=162$ ). The solid red line is the bias, and the dashed lines represent the 95% confidence interval.

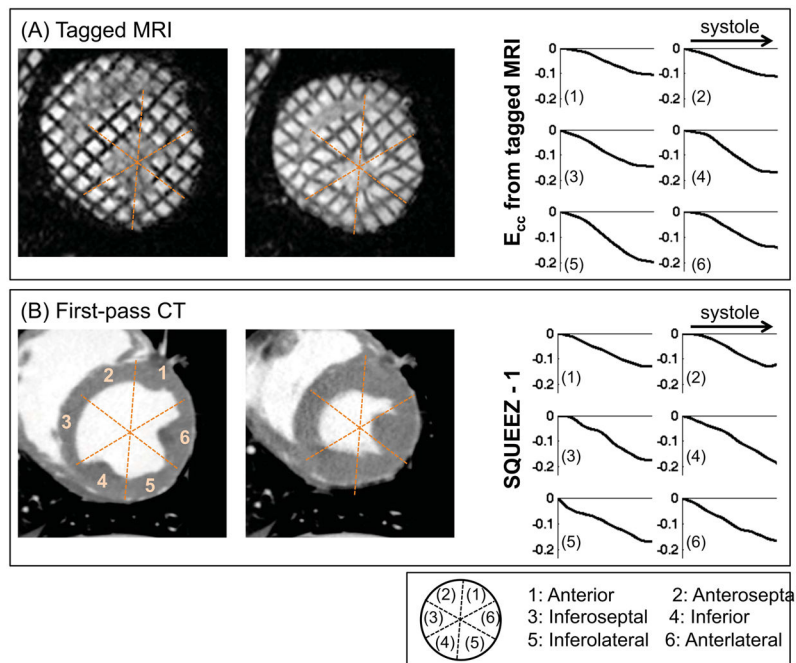


**Figure 4. Peak systolic function estimated from CT (SQUEEZ-1) and MRI ( $E_{cc}$ ) in 3 different myocardial regions**

No statistically significant difference was observed between the CT and MRI estimates within each region. The myocardial function showed statistically significant decrease starting from the remote region, to the PIZ, and to the MI region with  $p < 0.001$ .

**Table 1**

MRI acquisition parameters for the cine and tagged sequences.

	<b>Cine</b>	<b>Tagged</b>
<b>Sequence Type</b>	True-FISP	Gradient Echo
<b>Bandwidth (Hz/pixel)</b>	1000	185
<b>Repetition Time/Echo Time (ms)</b>	3.4/1.49	46.25/4.20
<b>Flip Angle (degrees)</b>	45	14
<b>Field of View (read (mm)/phase%)</b>	270/75%	270/65.6%
<b>Acquisition Matrix</b>	192 × 132	256 × 168
<b>Pixel size (mm)</b>	0.70 × 0.77	1.05 × 1.05
<b>Slice Thickness (mm)</b>	8	8
<b>Number of Slices</b>	8	8
<b>Echoes/Cardiac Phase</b>	6	9
<b>Cardiac Phases Per Slice</b>	32	13
<b>Parallel Imaging Factor</b>	2	n/a
<b>Grid Tag Spacing (mm)</b>	n/a	8

Author Manuscript

Author Manuscript

Author Manuscript

Author Manuscript

**Table 2****Ejection Fraction**

Ejection Fraction calculated from CT and Cine FISP MRI acquisitions for all animals.

Ejection Fraction		
Animal #	MR	CT
1	25	50
2	35	32
3	57	51
4	45	36
5	33	36
6	32	46
7	28	38
8	33	38
9	25	46

Author Manuscript

Author Manuscript

Author Manuscript

Author Manuscript